Applied Physics Letters

Blood coagulation monitoring under static and flow conditions with optical coherence tomography autocorrelation analysis

Cite as: Appl. Phys. Lett. **120**, 163702 (2022); https://doi.org/10.1063/5.0090725
Submitted: 08 March 2022 • Accepted: 07 April 2022 • Published Online: 19 April 2022

Yun Tang, Jiang Zhu, Lianqing Zhu, et al.

AIP Publishing

Applied Physics Letters ARTICLE scitation.org/journal/apl

Blood coagulation monitoring under static and flow conditions with optical coherence tomography autocorrelation analysis

Cite as: Appl. Phys. Lett. **120**, 163702 (2022); doi: 10.1063/5.0090725
Submitted: 8 March 2022 · Accepted: 7 April 2022 ·
Published Online: 19 April 2022

View Online Export Citation CrossMark

Yun Tang,[1,2] Jiang Zhu,[1,2,a)] Lianqing Zhu,[1,3,a)] Fan Fan,[1,2] Zongqing Ma,[1,2] and Fan Zhang[1,2]

AFFILIATIONS

[1]Key Laboratory of the Ministry of Education for Optoelectronic Measurement Technology and Instrument, Beijing Information Science and Technology University, Beijing 100192, China
[2]Beijing Laboratory of Biomedical Testing Technology and Instruments, Beijing Information Science and Technology University, Beijing 100192, China
[3]Beijing Key Laboratory of Optoelectronic Measurement Technology, Beijing Information Science and Technology University, Beijing 100192, China

[a)]**Authors to whom correspondence should be addressed:** jiangzhu@bistu.edu.cn and zhulianqing@sina.com

ABSTRACT

Detection of blood coagulation functions is essential for diagnosing blood diseases and treating vascular diseases. The viscoelasticity changes of the blood from a liquid to a clot can provide critical information for assessing blood coagulation. Here, we reported on noncontact monitoring of blood coagulation under static and flow conditions with optical coherence tomography (OCT) autocorrelation analysis. After OCT imaging, blood tissue dynamics were assessed by the OCT autocorrelation analysis during coagulation of the whole porcine blood. The properties of blood coagulation were quantitatively evaluated by three metrics, including the coagulation reaction time, the clot formation duration, and the maximum clot strength. The results show that the OCT autocorrelation method can quantify the coagulation properties under static and flow conditions and provides a unique opportunity for *in situ* coagulation detection and point-of-care testing.

Blood coagulation is a cascade process involving multiple stimulus responses for preventing the loss of excessive blood. Evaluation of blood coagulation functions can assist in diagnosing blood diseases and disorders, guiding the therapy of cardiovascular and cerebrovascular diseases, and assessing the risk of bleeding during surgery. The coagulation is accompanied by physical changes. Therefore, several physical measurements have been developed to monitor coagulation functions.[1]

Thromboelastography (TEG) and rotational thromboelastometry (ROTEM) can assess blood coagulation based on viscoelasticity measurements. However, the quantitative relationship between blood viscoelasticity and sensor motion is lacking, and clinical standardization needs to be established.[2,3] Optical coherence elastography (OCE) is an emerging optical imaging modality for characterizing biomechanical properties of soft tissues.[4–6] OCE can monitor the viscoelasticity during blood coagulation by measuring shear wave velocities and compressional wave attenuation.[7,8] The requirements of additional units for inducing mechanical waves in the blood increase the device complexity. A recently developed photoacoustic method can determine the viscosity of liquid blood by the flow speed measurement under constant pressure, which may have the potential for blood coagulation monitoring in the future.[9] Current coagulation detection based on the viscoelasticity measurements has not tracked clot formation in the flow state.

The measurement of flowing blood allows for a more accurate analysis of the blood coagulation process, because blood coagulation is dependent on states of blood flow in vessels.[10] The methods based on the measurements of light intensities may be used for the coagulation assessment under a flow condition. Nephelometry and turbidimetry can monitor blood coagulation by measuring the changes in light intensities.[11] The intensity attenuation associated with the refractive index mismatching between the plasma and the red blood cells has also been measured to assess the coagulation properties.[12,13] However, hemolysis, icterus, and lipemia could change the optical properties of the blood and distort the coagulation evaluation.

In this study, we developed an optical coherence tomography (OCT) autocorrelation method to quantitatively evaluate the coagulation properties under static and flow conditions. Benefitting from the sensitive, noncontact OCT measurements, the blood tissue dynamics were assessed to monitor the blood coagulation. The coagulation reaction time, the clot formation duration, and the maximum clot strength were quantitatively calculated under a static condition. Then the coagulation properties were assessed at different flow speeds in a capillary tube.

In a medium with nonspherical scattering particles, the tissue dynamics mainly consist of a slowly changing part due to random diffusion of the scattering particles, a rapidly changing part due to fluctuations of local pressure and temperature, and a rapidly changing part due to tumbling of the nonspherical particles (such as red blood cells).[14] The diffusion dynamics of the scattering particles are mainly related to the viscosity of the medium and the sizes of the scattering particles. In the liquid blood, the viscosity is relatively low, and the red blood cells are the dominant scattering particles. The small red blood cells undergo rapid motion, and thus, the liquid blood presents strong diffusion. During coagulation, the viscosity of the blood increases, and the red cell aggregates are the dominant scattering particles. The sizes of the scattering particles increase, and the particle motion slows down. The diffusion of the particles becomes weaker. Therefore, blood coagulation can be monitored by characterizing the diffusion dynamics.

Fourier domain OCT can detect the optical scattering signals with high sensitivity and high resolution and provides an efficient implementation of low-coherence interferometry.[15,16] The contrasts of the OCT signals are derived from the differences in the optical scattering properties. Incorporating the analysis of optical signals scattered by the moving blood cells, OCT can map the vascular network and quantify the blood flow.[17–20] OCT enables high-resolution detection of diffusion incorporating the dynamic light scattering analysis.[21] Using the M-scan OCT data, that is, repeated A-scans at a single lateral position, the autocorrelation of the scattering signals at an imaging depth z with a sequence length m and a time delay τ can be calculated by the following equation:[22]

$$A_s(\tau, z) = \frac{Cov[I(t,z) \times I(t+\tau, z)]}{\sqrt{Var[I(t,z)] \times Var[I(t+\tau,z)]}}, \tag{1}$$

where

$$Cov[I(t,z)\times I(t+\tau,z)] = \frac{\sum_{i=1}^{m}\left\{\left[I(t_i,z)-\frac{1}{m}\sum_{i=1}^{m}I(t_i,z)\right]\times\left[I(t_i+\tau,z)-\frac{1}{m}\sum_{i=1}^{m}I(t_i+\tau,z)\right]\right\}}{m}, \tag{2}$$

$$Var[I(t,z)] = \frac{\sum_{i=1}^{m}\left[I(t_i,z)-\frac{1}{m}\sum_{i=1}^{m}I(t_i,z)\right]^2}{m}, \tag{3}$$

and

$$Var[I(t+\tau,z)] = \frac{\sum_{i=1}^{m}\left[I(t_i+\tau,z)-\frac{1}{m}\sum_{i=1}^{m}I(t_i+\tau,z)\right]^2}{m}. \tag{4}$$

The OCT intensity sequences $I(t_i, z)$ and $I(t_i + \tau, z)$ are captured at the same lateral position but at a different time. The temporal decorrelation decay rate of the OCT intensity signals is sensitive to the tissue dynamics.[22] The decay rate in a short delay region is sensitive to the slow and rapid dynamics. Meanwhile, the decay rate in a larger delay region is sensitive to the slow dynamics.[22] To characterize the slow dynamics related to particle diffusion, the slope of the decorrelation decay is calculated in the larger delay region, which is defined as the decay constant D.

As the pig has a similar coagulation system to the human, porcine blood has been used as a standard model in coagulation research.[23] Fresh whole porcine blood was anticoagulated with sodium citrate. The whole blood sample of 2.5 ml was mixed with a $CaCl_2$ solution of 145 μl (12 g/l) and a saline solution of 100 μl to activate coagulation. The effects of the kaolin activation and the NaCl hemodilution on blood coagulation were assessed by the OCT autocorrelation method. In the kaolin effect test, the blood sample of 2.5 ml was mixed with a kaolin solution of 100 μl (20 g/l). Then the mixture was triggered to coagulation by a $CaCl_2$ solution of 145 μl (12 g/l). In the hemodilution test, the whole blood sample was diluted to 68% with 0.9% NaCl. The diluted blood sample of 2.5 ml was mixed with the kaolin solution of 100 μl (20 g/l), and then the mixture was triggered to coagulation by a $CaCl_2$ solution of 145 μl (12 g/l). After gently mixing for 1 min, the blood sample was loaded into a centrifuge tube for the coagulation measurements under a static condition. In the flowing blood tests, we prepared the same blood samples as those used in the kaolin effect test. Then the sample was injected into a transparent capillary tube for the measurements under flow conditions. Four repeated measures were performed in each group.

The system for the blood coagulation assessment is shown in Fig. 1(a). The OCT data were captured by a commercialized swept-source OCT imaging system (Model VEG210C1, Thorlabs, Inc., Newton, New Jersey). The wavelength of the swept-source is 1300 nm, and the A-line rate is 100 kHz. The axial resolution in the sample is about 10 μm.

In the static blood measurements, the blood sample of 1 ml was loaded into a centrifuge tube and was subsequently imaged by the OCT M-scans. Each M-scan consisted of 10 000 A-lines captured at a single lateral position, and the time interval between A-lines was 0.01 ms. The OCT M-scans were recorded every 10 s during the measurements. Figure 1(b) shows the M-mode OCT images at the beginning and the end of coagulation.

In the flowing blood tests, the blood sample of 2.5 ml was injected into a capillary tube with an inner diameter of 2 mm. Then the blood was driven to flow reciprocally by a syringe pump with an infusion time of 6 s, a stop time of 6 s, and a withdrawal time of 6 s. The flow rates were set to 1 and 2 ml/min. The OCT M-scans were recorded when the flow stopped. Each M-scan consisted of 10 000 A-lines at a single lateral position.

After the fast Fourier transform, the amplitude components of the complex sequence were extracted to analyze the autocorrelation. The series $I(t_i + \tau, z)$ was selected from 1st to 5000th A-lines ($i = 1, 2, \ldots, 5000$), and the time delay τ covered a range of 0–50.00 ms with an increase in 0.01 ms. The autocorrelation values were averaged within 100 pixels along the depth in the blood region.

The autocorrelation values A_s at different coagulation stages are shown in Fig. 2. When the time delay τ is very close to 0, $A_s(\tau)$ will be significantly affected by the rapid dynamics of the tissue, which are

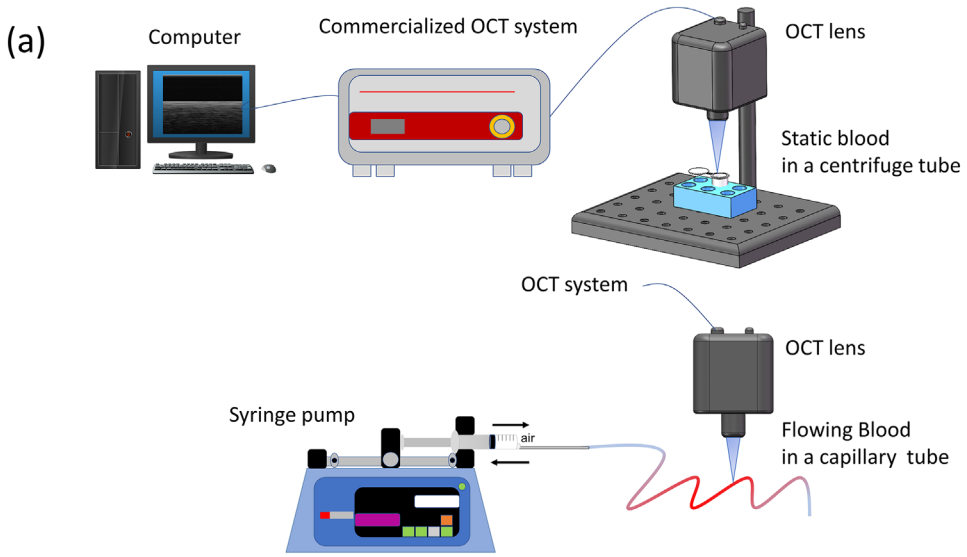

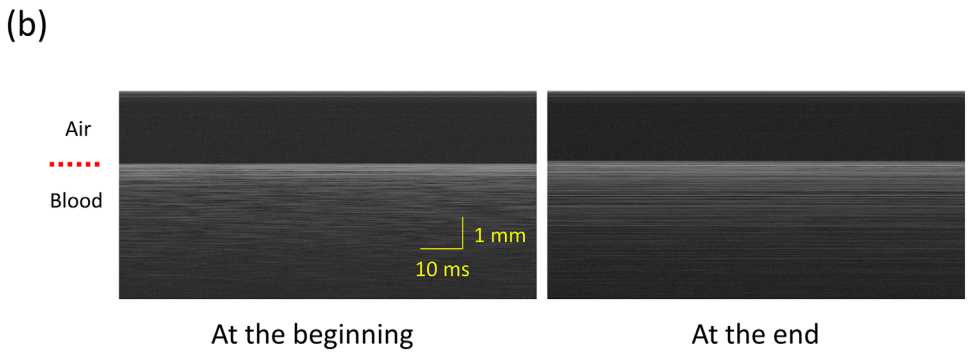

FIG. 1. The measurement system and M-mode OCT images for the coagulation assessment. (a) The measurement system under static and flow conditions. (b) M-mode OCT images at the beginning and the end of the coagulation under a static state.

caused by the fluctuations of local pressure and temperature, and the tumbling of the nonspherical particles. Therefore, the slope in a larger delay region of 2.00–5.00 ms was calculated by linear regression analysis. From Fig. 2, there is a significant difference in the slope between the liquid blood at the beginning of the coagulation and the blood clot at the end. Compared to the blood clot, the stronger diffusion of the small red blood cells causes a larger decay constant D in the liquid blood.

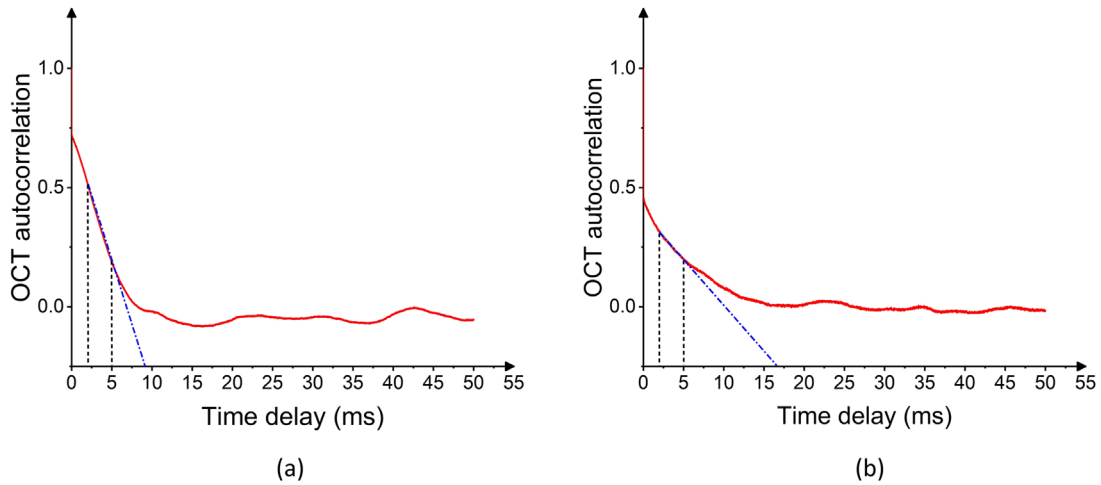

FIG. 2. Changes of the OCT autocorrelation A_s over the time delay τ at the beginning (a) and the end (b) of the coagulation process.

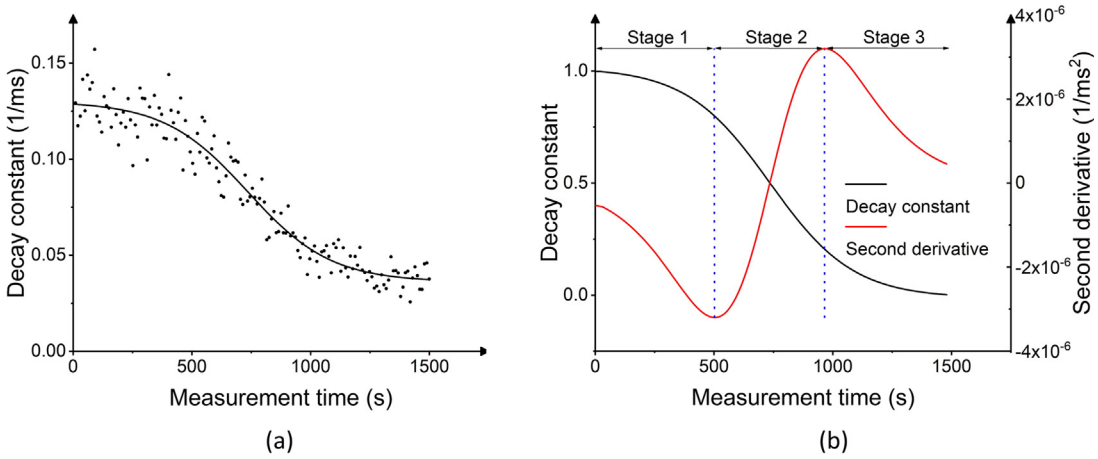

FIG. 3. Tracing and analysis of the decay constants during coagulation. (a) The plot of the decay constant vs the time after the whole porcine blood was triggered to clot. The plot was fitted into an S-curve. (b) Normalized S-curve and second derivative analysis. The maximum and minimum values of D are scaled to 1 and 0. The coagulation process was divided into three stages based on the second derivatives.

The decay constant D can be used to characterize the blood coagulation process. Figure 3(a) shows the plot of the decay constant vs the time after the static whole porcine blood was triggered to clot. From Fig. 3(a), three stages can be identified during blood coagulation. At the first stage, the diffusion is strong in a liquid status. During the second stage, the liquid blood turns rapidly into a blood clot. The increase in the blood viscosity and the aggregation of the red blood cells result in the weakening of the diffusion. At the third stage, stable blood clots have formed, and thus, the blood viscosity and the clot aggregation will not change significantly. The plot of the decay constant presents an approximately horizontal tendency.

Based on the three stages of coagulation, the plot of the decay constant is fitted into an S-curve in Fig. 3(a). Three coagulation metrics can be determined immediately by the analysis of the S-curve. The metrics can provide essential information on clot formation kinetics and clot strength. As the decay constants D are different at the beginning and the end of coagulation among the samples, the S-curve is normalized for convenient calculations in Fig. 3(b), where the maximum and minimum D values are scaled to 1 and 0. Subsequently, the second derivative of the normalized S-curve is analyzed. The occurrence time of the valley in the second derivative curve is defined as the coagulation reaction time. The interval between the peak and the valley in the second derivative curve is defined as the clot formation duration. The value of $1/D$ at the third stage is defined as the maximum clot strength. The coagulation reaction time, the clot formation duration, and the maximum clot strength, respectively, were 612 ± 91, 304 ± 83 s, and 25.08 ± 0.44 ms for the static whole blood without kaolin, as shown in Table I.

Then the OCT autocorrelation method was evaluated by the kaolin activation test and NaCl hemodilution test. Kaolin is an activator to trigger coagulation and can promote clot formation. Therefore, the kaolin can speed up the coagulation process and shorten the time of coagulation analysis. The NaCl hemodilution during the infusion therapy was validated to affect the coagulation process. Three groups of samples were compared, including the static whole blood without kaolin, the static whole blood with kaolin, and the static diluted blood with kaolin. The analysis of the decay constants in three samples is shown in Fig. 4(a). As the addition of kaolin resulted in rapid activation of the coagulation, the samples with kaolin were measured for 10 min instead of 25 min in the measurements of the samples without kaolin. From Fig. 4(a), the tracing can be fitted into an S-curve for each sample, and the coagulation process can be separated into three stages. The metrics of the coagulation reaction time, the clot formation duration, and the value of $1/D$ were compared in Table I.

After the addition of kaolin into the whole blood, the coagulation reaction starts much earlier, from 612 ± 91 to 235 ± 4 s ($P < 0.01$), and the clot formation duration is much shorter, from 304 ± 83 to 31 ± 4 s ($P < 0.01$). The change in the coagulation reaction time is consistent with the results from the OCE measurements and the TEG assays.[3,7] Unlike the elasticity measurements using the OCE,[7] the addition of the kaolin significantly shortened the clot formation duration according to our measurements, which may be partly caused by the

TABLE I. Coagulation metrics for different blood samples.

Blood sample	Coagulation reaction time (s)	Clot formation duration (s)	Maximum clot strength $1/D$ (ms)
Static whole blood without kaolin	612 ± 91	304 ± 83	25.08 ± 0.44
Static whole blood with kaolin	235 ± 4	31 ± 4	27.01 ± 0.39
Static diluted blood with kaolin	202 ± 11	39 ± 12	25.58 ± 0.33
Whole blood with kaolin at a flow rate of 1 ml/min	76 ± 5	37 ± 10	30.72 ± 0.61
Whole blood with kaolin at a flow rate of 2 ml/min	133 ± 8	44 ± 5	32.82 ± 0.76

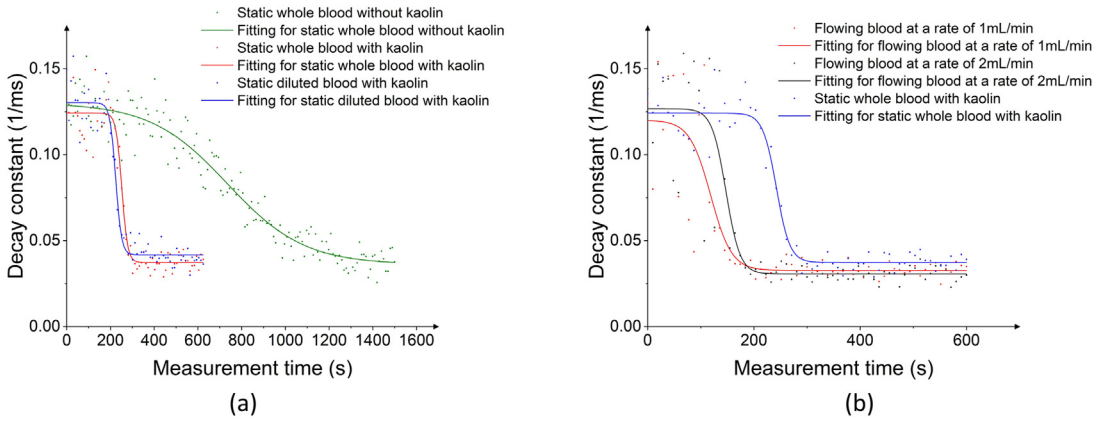

FIG. 4. Analysis of decay constants for static and flow samples. (a) Tracing and fitting of the decay constants for the static samples. (b) Tracing and fitting of the decay constants for the whole blood with kaolin under static and flow conditions.

asynchronous changes of the elasticity and the viscosity during coagulation. The increase in the value $1/D$ from 25.08 ± 0.44 to 27.01 ± 0.39 ms shows a slight rise in the maximum clot strength after adding kaolin into the whole blood ($P < 0.01$).

The influence of hemodilution was evaluated by measuring the static diluted blood and the static whole blood. The kaolin solutions were added to two groups of blood samples. After the hemodilution, the coagulation reaction time becomes a bit earlier from 235 ± 4 to 202 ± 11 s ($P = 0.02$); however, there is no difference in the clot formation duration ($P > 0.05$), which corresponds with previous viscosity-based coagulation measurements.[8] After the hemodilution, the $1/D$ value decreases slightly from 27.01 ± 0.39 to 25.58 ± 0.33 ms ($P = 0.03$), which indicates that the maximum clot strength decreases.

Finally, the effect of blood flow on coagulation was assessed. The whole blood with kaolin at the flow rates of 1 and 2 ml/min was compared with the static whole blood with kaolin, as shown in Fig. 4(b). The tracing of the flowing blood can be fitted to an S-curve. The metrics of the coagulation reaction time, the clot formation duration, and the value of $1/D$ are compared in Table I. At the flow rates of 1 and 2 ml/min, the coagulation reaction time are 76 ± 5 and 133 ± 8 s, respectively, which are much earlier than 235 ± 4 s ($p < 0.01$) in the static whole blood with kaolin. The blood flow accelerates the binding of the coagulation components and, thus, speeds up the clot formation. The coagulation reaction time delays from 76 ± 5 to 133 ± 8 s ($P < 0.01$) when the flow rate increases from 1 to 2 ml/min. There is a slight prolongation of the clot formation duration when the flow rate increases. The faster flow with higher shear stress has a stronger ability to break the fibrin meshwork and prevent enmeshing the red cells and plasma.[13,24] The maximum clot strength characterized by $1/D$ increases from 27.01 ± 0.39 in the static blood to 30.72 ± 0.61 ($p < 0.01$) in the flowing blood at a rate of 1 ml/min and further increases to 32.82 ± 0.76 ($p < 0.01$) in the flowing blood at a rate of 2 ml/min. The faster flow will help to form a blood clot with higher strength.[25]

We developed an OCT autocorrelation method for noncontact monitoring of blood coagulation under static and flow conditions based on the assessment of tissue dynamics. The method has three advantages compared to the previous coagulation assessment. First, blood coagulation can be assessed under flow conditions using our method. Conventional coagulation detection under a static state, such as the biochemical tests and viscoelasticity-based measurements, cannot follow the clot formation in the presence of the flow. The static blood in the container presents different coagulation properties compared with the flowing blood in vessels. The measurement of flowing blood with a similar status in vessels can analyze the blood coagulation more accurately. Second, coagulation can be monitored without contact, and thus, the OCT method has the potential for *in situ* detection in clinical applications. Noncontact detection can avoid contamination of the detection system from the blood samples. Third, coagulation can be monitored reliably without easily consumable units such as mechanical sensors and wave-induced actuators. The OCT autocorrelation method can improve the long-term reliability of the coagulation measurements. Some low-cost OCT systems have been developed, which makes the OCT systems cheaper with equivalent performance.[26] Therefore, the coagulation assessment with OCT autocorrelation analysis has prominent advantages and will be a valuable supplement to previous methods.

In this study, we developed an OCT autocorrelation method to assess the coagulation properties under static and flow conditions. Based on the analysis of the tissue diffusion dynamics, three stages were identified during coagulation from a liquid to a clot, and three metrics were proposed to provide essential information for the coagulation assessment. The results show that the OCT autocorrelation method can accurately characterize the coagulation properties of static blood and flowing blood. With noncontact and high-resolution OCT imaging, the method has the potential for *in situ* coagulation detection and point-of-care testing and, thus, will have significant impact on the diagnosis of blood diseases and the assessment of coagulation disorders.

This work was supported by grants from the National Natural Science Foundation of China (Nos. 61975019 and 61875237) and the Research Project of the Beijing Municipal Education Commission (No. KZ202011232050).

AUTHOR DECLARATIONS

Conflict of Interest

The authors have no conflicts to disclose.

DATA AVAILABILITY

The data that support the findings of this study are available from the corresponding authors upon reasonable request.

REFERENCES

[1]M. Mohammadi Aria, A. Erten, and O. Yalcin, Front. Bioeng. Biotechnol. **7**, 395 (2019).
[2]D. Bolliger, M. D. Seeberger, and K. A. Tanaka, Transfus Med. Rev. **26**(1), 1–13 (2012).
[3]D. Whiting and J. A. DiNardo, Am. J. Hematol. **89**, 228 (2014).
[4]B. F. Kennedy, P. Wijesinghe, and D. D. Sampson, Nat. Photonics **11**, 215 (2017).
[5]K. V. Larin and D. D. Sampson, Biomed. Opt. Express **8**, 1172 (2017).
[6]J. Zhu, X. He, and Z. Chen, Appl. Spectrosc. Rev. **54**, 457 (2019).
[7]X. Xu, J. Zhu, and Z. Chen, Sci. Rep. **6**, 24294 (2016).
[8]X. Xu, J. Zhu, J. Yu, and Z. Chen, IEEE J. Select. Top. Quantum Electron. **25**, 7200406 (2019).
[9]Y. Zhou, C. Liu, X. Huang, X. Qian, L. Wang, and P. Lai, Biomed. Opt. Express **12**, 7139 (2021).
[10]C. C. Huang and S. H. Wang, IEEE Trans. Biomed. Eng. **54**, 2223 (2007).
[11]M. A. O'Leary and G. K. Isbister, J. Pharmacol. Toxicol. Methods **61**, 27 (2010).
[12]X. Xu, J. Lin, and F. Fu, J. Biomed. Opt. **16**, 096002 (2011).
[13]X. Xu, J. Geng, and X. Teng, J. Biomed. Opt. **19**, 046021 (2014).
[14]B. J. Berne and R. Pecora, Annu. Rev. Phys. Chem. **25**, 233 (1974).
[15]*Optical Coherence Tomography: Technology and Applications*, 2nd ed., edited by W. Drexler and J. G. Fujimoto (Springer International Publishing, Cham, 2015), p. 3.
[16]Y. Zhou, J. Ni, C. Wen, and P. Lai, Theranostics **12**, 542 (2022).
[17]J. Zhu, C. W. Merkle, M. T. Bernucci, S. P. Chong, and V. J. Srinivasan, Appl. Sci. **7**(7), 687 (2017).
[18]J. Zhu, X. He, and Z. Chen, APL Photonics **3**, 120902 (2018).
[19]J. Liu, J. Zhu, L. Zhu, Q. Yang, F. Fan, and F. Zhang, J. Biophotonics **13**, e202000181 (2020).
[20]J. Zhu, B. Zhang, L. Qi, L. Wang, Q. Yang, Z. Zhu, T. Huo, and Z. Chen, Appl. Phys. Lett. **111**, 181101 (2017).
[21]J. Lee, W. Wu, J. Y. Jiang, B. Zhu, and D. A. Boas, Opt. Express **20**, 22262 (2012).
[22]I. Abd El-Sadek, A. Miyazawa, L. Tzu-Wei Shen, S. Makita, S. Fukuda, T. Yamashita, Y. Oka, P. Mukherjee, S. Matsusaka, T. Oshika, H. Kano, and Y. Yasuno, Biomed. Opt. Express **11**, 6231 (2020).
[23]J. L. Sondeen, R. de Guzman, I. Amy Polykratis, M. Dale Prince, O. Hernandez, A. P. Cap, and M. A. Dubick, Blood Coagul Fibrinolysis, **24**(8), 818 (2013).
[24]F. Shen, C. J. Kastrup, Y. Liu, and R. F. Ismagilov, Arterioscler., Thromb., Vasc. Biol. **28**, 2035 (2008).
[25]Z. Chen, J. Lu, C. Zhang, I. Hsia, X. Yu, L. Marecki, E. Marecki, M. Asmani, S. Jain, S. Neelamegham, and R. Zhao, Nat. Commun. **10**, 2051 (2019).
[26]G. Song, E. T. Jelly, K. K. Chu, W. Y. Kendall, and A. Wax, Prog. Biomed. Eng. **3**, 032002 (2021).